We are IntechOpen, the world's leading publisher of Open Access books Built by scientists, for scientists

4,800
Open access books available

122,000
International authors and editors

135M
Downloads

Our authors are among the

154
Countries delivered to

TOP 1%
most cited scientists

12.2%
Contributors from top 500 universities

CLARIVATE ANALYTICS BOOK CITATION INDEX INDEXED

WEB OF SCIENCE™

Selection of our books indexed in the Book Citation Index in Web of Science™ Core Collection (BKCI)

Interested in publishing with us?
Contact book.department@intechopen.com

Numbers displayed above are based on latest data collected.
For more information visit www.intechopen.com

7

Acute Coronary Syndrome: Pathological Findings by Means of Electron Microscopy, Advance Imaging in Cardiology

Mohaddeseh Behjati[1] and Iman Moradi[2]
[1]*Isfahan University of Medical Sciences,*
[2]*NCDC Center,*
[1]*Iran*
[2]*Italy*

1. Introduction

Acute coronary syndrome (ACS) caused by a blockage in coronary arteries as a result of atherosclerosis or thrombosis, is one of the leading causes of death worldwide [Rajapakse et al., 2010]. Due to the altered trends of ischemic heart disease and emergence of some new cardiovascular risk factors in depth understanding of the underlying pathophysiological mechanisms is needed. In this way, inspection of the anatomical structures responsible for the development of acute coronary events is highly deemed and electron microscope is the right instrument for this purpose.

For a long while, electron microscopy has been used as one of the best instruments for pathologic diagnostics. These scientific instruments use a beam of highly energetic electrons to examine objects on very fine scales. Limitations of light microscopes due to the physics of light with limited 500X or 1000X magnification and a resolution of 200 nanometer let scientist to search for development of Electron Microscopes. Basic steps involved in all EMs, regardless of type, include a stream of electrons made by electron source which is accelerated toward the specimen using a positive electrical potential. This stream is restricted and focused into a thin beam using metal apertures and magnetic lenses. Electron beams are affected by interactions occurred inside the irradiated sample. These interactions are transformed to the final image [www.upesh.edu.pk].

Transmission Electron Microscope (TEM) was the first type of Electron Microscope developed by Max Knoll and Ernst Ruska in Germany in 1931. It was patterned exactly on the Light Transmission Microscope except application of a focused beam of electrons instead of light in order to "see through" the specimen. TEM functions with a high voltage electron beam in order to create images [McMullan, 1993]. Emitted electrons by electron gun fitted with a tungsten alloy filament cathode as electron source. An anode typically at 100 KeV accelerates electron beams with respect to the cathodes, are focused by electrostatic and electromagnetic lenses and transmitted through the specimens. Thus, scattered electron beams carries information about the structure of specimen which is magnified by objective lens system of microscope. The final image will be appeared on a screen coated by

fluorescent material. This specific screen is necessary as the regular images of electrons are not visible for our eyes. Images detected by CCD (charge-coupled devices) camera might be displayed on a monitor or computer [Wikipedia]. The resolution of TEM is partly limited by spherical aberrations but using aberration correctors, achievement of higher resolutions became possible. This correction using hardware made it possible to achieve images with resolution values below 0.5 angstrom and magnifications above 50 million times by for high-resolution TEM (HRTEM) [Erni et al., 2009, Wikipedia].

Freeze-fracturing also known as freeze-etch or freeze-and-break is another preparation method valuable for evaluation of lipid membranes and their incorporated proteins in "face on" view [Severs, 2007, Sekiya et al., 1979]. It reveals proteins embedded in lipid bi-layer [Sekiya et al., 1979]. Fresh tissue or cell suspension is frozen promptly (cryofixed), then fractured by simple breaking or using a microtome at liquid nitrogen temperature [Osumi et al., 2006, Dempsey & Bullivant, 1976]. Cold fractured surface is consequently "etched" by increasing the temperature to about -95°C for a few minutes, in order to reveal microscopic details by subliming surface ice. One rotary-shadowed with evaporated platinum at low angle (typically about 6°) in a high vacuum evaporator is required for TEM as an extra- step that is not needed for SEM. To improve the stability of replica coating, a second carbon coating is generally performed. Thereafter, chemical digestion with acids, hypochlorite solution or SDS detergent is used to release the extremely fragile "shadowed" metal replica of the fracture surface. Washed floating replica is picked up on EM grid and used for TEM evaluation after complete drying [Wikipedia]. Freeze-etched preparation of vessels can be investigated using this method to demonstrate altered intimal cushions in cases with and without ACS. Immune localization study of deep-etch replicas of frozen vessels will enhance our knowledge regarding pathologic changes during the process of ACS development. This method is highly suitable for depiction of fat deposits in vessel walls (Guyton & Klemp, 1992). Actually, the hypothesis of fused lipoproteins in the extracellular space to form larger lipid deposits has been first proposed by Frank and Fogelman using this technique [Guyton & Klemp, 1992].

Scanning Electron Microscope (SEM), first debuted around 1965, works exactly as their optical counterparts except using a focused beam of electrons rather than light to image specimens and gain informatics details about their composition and structure. It images samples by scanning it with high-energy electron beams in a raster scan pattern. Signals made by interaction of electron beams with samples' atoms bring information about the sample's surface topography, composition, and other properties as electrical conductivity. The final image resolution of SEM is poorer than that achieved by TEM. Since SEM images rely on surface processes rather than transmission, bulk imaging of samples up to many centimeters in size with great depth of field is possible. Thus, images with good representation of three-dimensional shape of samples can be achieved [Wikipedia]. SEMs equipped with cold stage for cryo-microscopy can be used for cryofixation as low temperature SEM [Read & Jeffree, 1991]. Cryo-fixed specimens can also be cryo-fractured under vacuum to reveal internal structures [Faulkner et al., 2008]. Sputter coated cryo-fractured specimens are transferred onto cryo-staged SEM in frozen state [Faulkner et al., 2008]. Low-temperature SEM can be used effectively for imaging temperature-sensitive materials as fats, thus fatty athermanous plaques might be good subjects for this kind of imaging [Hindmarsh et al., 2007].

One of the fundamental progresses in the field of SEM has been related to the development of environmental scanning electron microscope (ESEM). Since conventional SEM needs high vacuum for proper imaging, samples that produce significant amounts of vapor like wet or oily biological samples need to be either dried or cryogenically frozen. ESEM developed in late 1980s, allowed samples to be observed in high relative humidity and low-pressure gaseous environments [Mohankumar, 2010]. This capability has been attributed to the presence of secondary-electron detectors operating in the presence of water vapor and pressure-limiting apertures supplemented with differential pumping in the path of electron beams in order to separate vacuum region from the sample chamber [Mohankumar, 2010]. Bypassing the need for coating with carbon or gold, ESEM became a useful instrument for investigation of non-metallic and biological materials [Ishidi et al., 2011]. Irreversibility of coating process with concealing effects on sample surface might reduce value of obtained results and the advantage of ESEM is bypassing this step [Ishidi et al., 2011]. In contrary with SEM, ESEM allows X-ray microanalysis on uncoated non-conductive specimens [Wikipedia]. In this case, polymer or surface damage induced after intravascular deployment of drug eluting stent has been visualized using ESEM [Wiemer et al, 2010]. Indeed, evaluation of qualitative surface morphology and elemental analysis of intravascular stents designed for the treatment of ACS is possible through ESEM [Sojitra et al, 2009]. Despite of these advancements, there is still plenty room for further applications of ESEM in revealing the underlying pathophysiological mechanisms of ACS.

Meanwhile, SEM plays a main role in characterization of athermanous lesions containing oily and volatile materials through a new approach called wet SEM technique. It is ideal for examination of fully-hydrated or liquid-containing samples – as biological cells, tissues, and fluid suspensions [Bergmans et al., 2005]. Wet SEM technique provides researchers by an accurate and detailed structural evaluation of pathological processes involved in development and progression of atherosclerosis [KAMARI et al., 2008]. In wet SEM, wet samples are protected from high vacuum conditions applied in conventional EMs [Bergmans et al., 2005]. Conventional EMs, need samples to be evaluated at high vacuum conditions, wet specimens are not suitable for evaluation using this today's primary tool for high-resolution imaging. This is one major drawback for application of EM in biomedical research. Previously, wet specimens were evaluating using freezing or drying. This time-consuming, costly and artifact-prone procedure was associated with changing specimen's nature and consequently. Wet SEM has reduced the preparation needs required for high-resolution of such wet specimens which consequently made easier and faster imaging possible. Less occurred artifacts are also note worthy. This technique is cheap and widely applicable for various samples [Bogner et al., 2007].

Other developed EM variations are also useful for investigation of ACS, which are included here. EM-immunohistochemistry serves in distinct subcellular localization of proteins in heart as at the level of sarcomer, A-, I-, H- bands and Z-, M-line. It needs labeling of ultrathin sections with purified polyclonal antibodies. This helps in understanding the cell function in normal and pathologic conditions. Immune gold EM is based on the application of antibodies against the desired element and densities of immune labeling reflected by number of gold particles per unit area of respective structural component. It has been applied for determination of proteins in myofibrils associated with actin, myosin filaments and with sarcomers (Z-lines), in sarcoplasmic reticulum and in mitochondria [Maco et al., 2001].

EM-TUNEL serves a fundamental role in definite distinguishing apoptotic cells and their remnants from necrosis. Indeed, it can detect apoptotic cell death without nuclear condensation or DNA fragmentation. Immune gold particles in normal cells are slightly accumulated on nuclear heterochromatin, contrary with apoptotic cells in which gold particles are significantly accumulated on condensed chromatin. Due to high electron density of apoptotic nucleolus, fainter prints with attenuated contrast of background are recommended. Evaluation of myocytes and smooth muscle cells (SMCs) isolated from primary coronary lesions using EM-TUNEL showed rich glycogen granules in cytoplasm, condensated chromatin clumped to the nuclear envelope with clearing of central nuclear region, fragmentation of internucleosomal DNA, cell fragmentation into small membrane-bound vesicles in the presence of undamaged mitochondria and without rupture of cell membrane at early stages [Ohno et al., 1998]. Matrix vesicles also known as apoptotic detritus vary in size and shape but are often speckled appearance reflect final phase of apoptosis [Bauriedel et al., 1999]. Cell shrinkage, subsequent formation of membrane bound apoptotic bodies and phagocytosis are observed in final stages [Ohno et al., 1998].

For biological specimens, sample preparation is necessary. Inside the electron microscope is under high vacuum suitable for travelling of electron beams in a straight line which makes sample processing a prerequisite step. Applied processing procedure highly depends on the specimen, mentioned analyses and type of applied microscope. The quality of final electron micrograph is a function of the quality of preparation. EM is an expensive technique due to the complexity of process and the cost of applied materials, but it is still profitable because of its power for diagnostics purposes. Biological specimens should be dried completely for evaluation under high vacuum condition of SEM. Living cells, tissues and soft-bodied organisms often need chemical fixation prior to preservation and stabilization of their structure. For evaluation of pathologic and reparative alterations during ACS, samples taken from infarcted regions, periinfarct site regions bordering the infarction, are at risk, the center of non-risk area, subendocardial, subepicardial or transmural portions and healthy tissue in the left ventricular myocardium or anterior superior intraventricular septum as positioning control samples are valuable. Samples could be taken using paunch biopsy or by cutting the region of interest under direct visualization, based on the characteristics of the sample source. Transmural biopsies could be taken during coronary intervention, percutaneous atherectomy or bypass graft surgery. Obviously, direct tissue sampling from heart can be achieved through post-mortem analysis of research animal models or expired humans suffered from ACS. Samples should be taken immediately after killing animals. In addition to myocytes, coronary arteries can also be evaluated after AMI by subdividing them into infarct related artery (IRA) and non –IRA. Stenotic segments can be cutted and decalcified if necessary. Animal models of acute ischemia and ischemia-reperfusion injury (wild type or knocked-out and transgenic) facilitated these kinds of investigation, especially in the case of evaluation of temporal changes after ACS. Models of temporarily ischemia, reversibly vs. irreversible injury, gentle vs. abrupt reperfusion and other intended study models can be generated in vivo. Animal hearts can be fixed with vascular perfusion of fixative agents through abdominal aorta. Perfusion fixation allows usage of vascular system of a deeply anesthetized animal to deliver fixative agents to tissues of interest. Since tissues are fixed before autolysis begins, this technique is considered as the optimal method of tissue preservation. Perfused tissues are less vulnerable to artifact injuries caused by handling. Fixation techniques vary depending on the organ, tissue and the desired

processing. Appropriate literature review should be done to determine the ideal technique for the organ of concern. With perfusion fixation in contrast to direct immersion fixation, no cell rupture during mincing prior to fixation will occur.

Immediately fixed cardiac endothelium presents an invariable surface throughout the interior of the heart. Smooth predominant nuclear bulges and attenuated peripheral plasmalemma with occasional marginal ruffles, scattered microvilli and small blebs can also be seen. Various stages of systole and diastole lead to some physiological local variations in SEM of endocardium. Great liability of endocardial surface is seen in response to classic "holding solution" often used in preparatory technique. Thus, caution must be paid in preparing soft tissues for SEM in the case of applied "holding solution" [Peine & Low, 1975]. Some tissues need pretreatment before fixation step, as SMCs which should be collected after trypsinization [Tran et al., 2004].

Harvested samples should be immediately transferred to cold fixative agent. Samples can also be freezed rapidly, typically to liquid nitrogen temperatures or below, that water forms ice (cryofixation) [Mitsuoka, 2011]. This preserves the specimen with the minimal of artifacts. With cryo-electron microscopy, it is possible to observe any biological specimen close to its native state. Anyway, preserved samples are then dissected into small cubes when lying in the fixative and fixed. Fixation is a general term used to describe the process of preserving a sample at a moment in time and to prevent further deterioration so that it appears as close as possible to what it would be like in the living state, although it is now dead. Fixation is performed by incubation of samples in a solution of a buffered chemical aldehyde-based fixative, such as glutaraldehyde, paraformaldehyde, or formaldehyde or combinations of these [Read & Jeffree, 1991, Karnovsky, 1965, Kiernan, 2000]. For primary fixation, glutaraldehyde buffered (pH 7.4) in sodium cacodylate, Sucrose or phosphate buffers (PBS, HEPES, and PIPES), are used. Glutaraldehyde and osmium tetroxide are often used to crosslink protein molecules and to preserve lipids, respectively. This step is followed by post-fixation with osmium tetroxide (OsO4) [Read & Jeffree, 1991]. A buffer containing sodium cacodylate, Sucrose and 2-Mercaptoethanol is recommended if precipitation is visible in final sections. Secondary fixation with OsO4 can be performed either in aqueous or in the same buffer as used in the primary fixative. Osmium-based procedures should be performed under a fume hood with worn gloves due to the toxicity and fixation capability of the Osmium fumes. Aqueous Uranyl acetate can be used for tertiary fixation or en-bloc staining. This can enhance membranes preservation by serving both as a fixative and stain. Fixed tissues are then dehydrated in graded series of ethanol or through using an acetone gradient or propylene oxide. It is a stepping stone towards total drying infiltration with resin for subsequent embedding for SEM or TEM analysis, respectively. Samples are treated with propylene oxide in a mixture of EM grade resin and Succinic anhydride as the transition solvent before embedding. Samples are then embedded in an adhesive such as epoxy resin, EPON medium, Spurr's Resin, LR White and so on.

Since air-drying causes sample collapse and shrinkage, critical point drying (CPD) is used commonly for dehydration step. CPD replaces intracellular water with organic solvents as acetone. These solvents replace in turn with a transitional fluid as liquid carbon dioxide at high pressure. By removing of carbon dioxide in a supercritical state, no gas-liquid interface will be present within the sample during drying [ProSciTech]. After heat polymerization, ultrathin sections, typically under 90 nm, which are semitransparent to electrons, are

preferred. Using ultramicrotomes or diamond knives, these sections are prepared from selected blocks. Glass knives and are much cheaper than diamond and can be easily made in laboratory, but they blunt frequently and need replacing. Optimal timing of serial sectioning after AMI should be kept in mind. After 24 hrs the edges of infarct becomes very narrow and easily missed on biopsy specimens [Hoffstein et al., 1975]. In contrast, biopsy specimens from marginal zones are easily taken in early hours after AMI [Hoffstein et al., 1975]. For SEM, sample size must be considered due to limitations of microscope chamber size and specimen exchange. Sections are then collected on metallic grids. Grids are mesh-like metallic discs for holding the ultrathin sections. The number of meshes varies from one for calibration of instrument to 1000 for studying the viruses. Therefore, the number of meshes depends on the size of specimen and accuracy of the study. For tissues like athermanous plaques and heart we recommend 200-mesh grids which may be made of gold, Nickel, silver, copper or other conductive metals. In SEM, dry specimens are usually mounted on stubs using electrically-conductive double-sided adhesive tape. Tissues are stained with the salt of Uranyl acetate and followed by lead citrate in double staining. Experimentally, Uranyl acetate provides better membrane perseveration and contrast but it leaves empty spaces in cells due to glycogen extraction [Vye & Fischman, 1970]. Indeed, the acidic pH of the stain leads in calcium extraction which subsequently results in un-visualization of mitochondrial granular dense bodies using en blocks stained it aqueous Uranyl acetate [Kloner et al., 1974].

Since biological samples are nearly transparent to electron beams, heavy metals give contrast between different structures by scattering imaging electrons. By staining using heavy metals, added electron density results in better contrast by providing more interaction between primary beam and those of sample. Then, samples are sputter coated using electrically-conducting materials, deposited on the surface of samples by low vacuum coating, in order to prevent specimen charging during imaging process due to accumulation of static electric fields by irradiated electrons. In this way, the amount of detectable secondary electrons from the surface of samples and consequently signal to noise ratio are increased [Mancuso et al., 1988]. Generally, gold or gold alloys, silver and iridium are used for this purpose [Suzuki, 2002]. Gold with high atomic number provide a coating with high topographic contrast and resolution [Wikipedia]. However, this coating with a few nanometer thicknesses can obscure the underlying through details of samples at very high magnification. Imaging without coating has been possible using low-vacuum SEMs with differential pumping apertures [Schatten & Pawley, 2007]. Thus, coating induced loss of contrast is obviated but the obtained resolution will be less than SEM with conventional sample coating [Schatten et al., 2008]. Ultimately, processed samples undergo observation and photography using a perspective electron microscope. Attention should be paid regarding possible loss of agents from tissues during fixation and embedding.

Due to the complexity of sample preparation, a technique so-called cryoultramicrotomy facilitates this process. Cryofixation, cryoultramicrotomy, and appropriate transfer of cryosections into the electron microscope are vial for proper ultrastructure and measurement of subcellular elemental distributions [Hagler et al., 1986]. All of these stages seem fundamental for experimental analysis of ultrastructural modification of heart prior, within and after acute ischemic insult. In cryo-ultramicrotomy or cryo-sectioning samples are sectioned at temperatures below 273K in order to avoid damaging effects of

temperatures above this threshold on ultrastructure by lipid melting [Hagler et al., 1986]. Rapid section freezing leads to occurrence of minimal or no ice damage during the cryofixation step. Hagler et al., 1986]. This technique facilitates the process to cut objects, hardened by cooling, without the need for deleterious fixation, dehydration, and embedding. In this way, a favorable basis for x-ray microanalysis of electrolytes and soluble cell constituents and histochemical and immunocytochemical localization of molecules is gained from frozen sections. But this technique is not confined to frozen sections and non-aqueous components embedded in a water matrix can also be used. Preparation of plastics, polymers, and elastomers either liquid or highly flexible at ambient temperatures is allowed by technique. Mechanical strength of object has been increased by applied low temperature which is associated with attenuated viscosity and plastic flow. It will convert essentially liquid materials to solids, if enough low temperature is reached [Adelide University, 2011]. An important issue which should be cared while handing with cryoultramicrotomy and cryo-sectioning, is proper cryotransfer stage for transfer of sectioned pieces from cryoultramicrotome to the electron microscope [Hagler et al., 1986]. By application of this stage, potential problems with rehydration damage to freeze-dried sections are avoided [Hagler et al., 1986]. Indeed, possible lipid melting in sections is also prohibited [Hagler et al., 1986]. In this way, tissue morphology and *in situ* elemental distribution are well preserved within tissues [Hagler et al., 1986].

Since tissue antigenecity is preserved using cryo-ultramicrotomy, this technique is suitable for in-depth investigation of mechanisms involved in the pathogenesis of ACS [Russell. et al., 1998]. This technique has been previously used for structural analysis of cardiac muscle [Luther, 2007]. Cryoultramicrotomy of myocardium using a cryosystem interfaced with an ultramicrotome was performed by BUJA et al to investigate microanalysis of the elemental composition of rabbit myocytes in hypoxic conditions. In this study, a knife temperature as low as -100^0C was applied [Buja et al., 1983]. Substructure of inner mitochondrial membranes of myocardial cells has also been depicted using cryo-ultramicrotomy [Sætersdal et al., 1978]. This technique can provide good facilities for depiction of ultrastructural modifications during the process of development and progression of ACS.

Depiction of some sub-cellular elements needs more manipulation. Mitochondrial pellet preparation is partly a complex process. Heart pieces after mincing with scissors are immersed and homogenized in isolation buffer containing sucrose, mannitol, EDTA in Tris/HCL pH 7.4. For optimal homogenization, tissue grinder can be used. Supernatant of centrifugated homogenate is poured through cheesecloth, re-centrifugated and re-suspended in above buffer. Mitochondria are washed in that buffer and centrifugated. Isolated mitochondria are stored on ice prior investigation [Bopassa et al., 2006]. For depiction of ribosomes, residual glycogen storage should be extracted [Vye & Fischman, 1970]. Evaluation of glycogen content is performed using PAS-staining [Sherman et al., 2000]. Masson tri-chrome staining can be used for collagen staining [Toumpoulis et al., 2009].

Acute coronary syndrome is mainly evolved from insidious development of atherosclerotic nidus. Each plaque is composed mainly from a fatty core, a fibrous cap with partly calcified shell. It is the proportion of fatty core to the fibrous cap that determines the plaque stability. Using SEM, cholesterol crystals (CCs) with intima perforation and tearing have been demonstrated within plaques prepared with ethanol or vacuum dehydration [Abela et al.,

2009]. Cholesterol crystals vary in shape and size, perforating the intima of coronary arteries and are strongly associated with acute coronary syndrome and cardiac death as well as with thrombus at rupture and/or erosion sites [Schmid et al, 1980, [Ewence et al., 2008]. This suggests that cholesterol crystallization is critical to plaque rupture and/or erosion and is associated with thrombosis and clinical events [Abela et al., 2006]. Cholesterol materials expand with crystallization tearing and perforating fibrous tissues [Abela et al., 2009]. Acute coronary syndromes are mainly attributed to plaque rupture or erosion [Sun et al., 2011]. Thus, plaque morphology determines plaque phenotype. These events are commonly known as plaque disruption (PD) [Abela et al., 2006]. The role of CCs in triggering and development of PD is yet unknown. Recently, it has been observed that large plate-like calcified areas are correlated with stable plaque phenotype [Ewence et al., 2008]. In contrary, speckled or spotty calcified deposits are commonly observed in ruptured atherosclerotic plaques [Virmani et al., 2003, Ehara et al., 2004, Vengrenyuk et al., 2006]. It has been suggested that microcalcifications exert local stress in atherosclerotic fibrous caps [Virmani et al., 2003, Ehara et al., 2004, Vengrenyuk et al., 2006]. Calcium phosphate micro- and nanoparticles and hydroxyapatite-containing "atherosclerotic gruel" lead to apoptosis of plaque vascular SMC (VSMCs) which is linked with weakening of the fibrous cap and plaque rupture and instability [Ewence et al., 2008]. Multiplication of SMC nuclei have been observed in atherosclerotic plaques, but SMCs "hurry on to their own destruction" as Virchow has stated, which brings plaque instability [Virchow, 1860]. SEM evaluation of calcified extracts from ruptured plaques demonstrated that small non-aggregated particles are more cytotoxic to VSMCs than larger deposits [Ewence et al., 2008]. Indeed, small crystals are more potent than large ones in activating inflammatory cascades driven by macrophages [Nadra et al., 2008]. Calcium phosphate crystals lead in rapid rise in intracellular calcium ion concentration [Ewence et al., 2008]. Un-sequestrated calcium leads to loss of function of membrane pumps and consequently cell death [Ewence et al., 2008]. VSMC death potentiates calcification by providing a nidus for further nucleation and activation of various downstream inflammatory pathways as release of cytokines [Proudfoot et al., 2000, Park et al., 2006, Zhou et al., 2008, Porto et al., 2006]. In addition to size, crystal composition is also of paramount importance. Similar effects in reducing VSMC viability was seen by synthetic carbonated or noncarbonated forms of hydroxyapatite [Ewence et al., 2008]. Hydroxyapatite crystals are found to be less damaging than more soluble forms of calcium phosphate [Ewence et al., 2008]. In this regard, analytic EM played a great role. Analytical EM clarifies the correlation of structure and elemental content in thin sections of normal and diseased tissues [Buja et al., 1976]. Through detection of specific elemental traces, it helps in localization of histological reactions [Buja et al., 1976]. Subtle changes of electrolyte homeostasis can be identified through this technique [Buja et al., 1976]. Indeed, cryo-ultramicrotomy techniques for preparation of unfixed, unstained thin section allow elucidation of very early stages in formation of calcium-containing inclusion bodies [Buja et al., 1976].

Other factors as surface crystal properties and containing factors like anti-apoptotic and calcification-regulatory proteins as fetuin might attenuate their detrimental effects [Ewence et al., 2008]. In design of research on the mechanisms of plaque calcification and identification of treatments to ameliorate plaque calcification, it should be kept in mind that tissues should be prepared without ethanol solvents that dissolve CCs, are highly recommended [Abela et al., 2009]. Accumulated calcium in tissues leads to mitochondrial

damage and prevention of cell recovery [Duchen, 2004]. SEM analysis of fixed mitochondrial suspension demonstrated opening of mitochondrial transition pores in response to calcium-induced permeability [Hüser et al., 1998]. This mitochondrial damage is associated with formation of two types of mitochondrial inclusion bodies as necrotic cell type inclusion and viable cell type inclusions. The former which occupies enlarged matrix spaces, masks crista membrane profiles and often invaded intracristal spaces of disrupted mitochondria has been observed in aneurysmal ventricular wall. The second type of inclusion materials occurred in the presence of various focal ultrastructural changes has been observed in hearts with old myocardial infarctions or unstable angina [Kawamura et al., 1978].

Typical phenotypic characteristics of normal fixed cardiomyocytes revealed by SEM and TEM include ovoid nucleus with irregular shallow indentation and evenly distributed nuclear chromatins with small amounts of heterochromatin clustered near inner nuclear envelope, regularly ordered myofibrils with intact sarcolemma, contracted sarcomers, prominent I bands, intact intercalated discs with narrow interspaces and regularly patterned honeycombs of sarcoplasmic reticulum over the periphery of myofibrils are observed [Sherman et al., 2000, Sage & Jennings, 1988]. In addition, lysosomes with variable amounts of lipid and dense materials, dense granules of glycogen particles distributed through the cell mainly in perinuclear regions, abundant mitochondria elongated between myofibrils, rounded in perinuclear areas with intact double membrane, numerous tightly packed orderly cristae, small condensed homogenous matrix space and tiny dense randomly scattered intra-mitochondrial matrix granules are also visible [Sherman et al., 2000, Li et al., 2001, Sage & Jennings, 1988]. Patent and empty capillaries with few collagen fibers in a relatively clear matrix are other findings in normal myocytes [Sage & Jennings, 1988].

In myocytes suffered from ischemic or reperfusion injury SEM and TEM analyses marked intracellular and extracellular edema, parenchymal cell swelling, hemorrhage, endothelial cell swelling, intraluminal bleb formation, disappeared Lysosomal enzymes from lateral sacs of vesiculated sarcoplasmic reticulum, disintegrated sarcolemma membrane, appearance of electron dense materials in capillary lumen, membrane-bound vesicles disintegrated plasma membrane, partial or complete depletion of glycogen granules, nuclear chromatin indentation are identified [Sherman et al., 2000, Sage & Jennings, 1988, Hoffstein et al, 1975]. In swollen cells contraction bands with few thick filaments in the A band and disarrayed sarcomers with preferential loss of myosin thick filaments, relaxed I bands, some hypercontractile areas in adjoining "unaffected" myocytes, abnormally contracted myofibrils, disrupted myofibrils with interfilamental edema and large intracellular vacuoles are apparent [Sage & Jennings, 1988, Sherman et al., 2000]. Empty electron lucent spaces seen between myofibrils around mitochondria and free cell margin are attributed to the appearance of wide clear interstitial spaces separating myocytes [Sage & Jennings, 1988]. Large subsarcolemmal bleb-like fluid spaces, possibly derived from dilated sarcoplasmic reticulum, appear tom compress adjacent capillaries [Sherman et al., 2000, Sage & Jennings, 1988]. In ischemic tissue, collapsed vessels with reduced capillary lumen are visible [Sage & Jennings, 1988].

Presence of normal or slightly damaged mitochondria in cells with severely injured cytoplasm implies the occurrence of mitochondrial damage subsequent to cytoplasmic damage [Hoffstein et al., 1975]. Spectrum of inspected mitochondrial changes seen using

SEM, TEM and STEM during AMI include denudation of mitochondrial structure as well as reorganized and processed mitochondria with mitochondrial swelling, loss of matrix density, formation of large annular, granular and amorphous intramitochondrial dense bodies, mitochondrial calcification, complete loss of tubular cristae (cristolysis), extensive swelling and appearance of mitochondria containing mitochondria remnants [Kloner et al., 1974, Buja et al., 1976]. No trace element was detected in moderately electron-dense amorphous inclusion bodies in mitochondria isolated from centers as well as the peripheries of myocardial infarcts [Buja et al., 1976]. Appearance of flocculent granules or "amorphous matrix" within mitochondrial cristae reflects server irreversible mitochondrial injury as a result of precipitation of denatured proteins [Buja et al., 1976].

In spite of plaque composition, EM evaluation could be applied to display other players in evolution from stable plaque to ACS. Inflammation is a tightly bound element to the progression of stable towards unstable plaques. Leukocyte margiantion and migration into nascent atherosclerotic plaques are correlated with severity of atherosclerosis and extent of endothelial cell turnover [Jerome et al., 1983]. The sites of rapid endothelial cell turnover with enhanced leukocyte adherence were depicted using stereological analysis of conventional SEM preparations [Jerome et al., 1983]. Although accumulation of leukocytes and inflammatory cells occurs in area susceptible to atherosclerosis, critical congestion of these cells is particularly evident at the growing edge of lesions [Jerome et al., 1983].

Another participant factor in the scenario of ACS is activation of thrombotic cascades. Thrombus formation occludes capillary lumen at the site of plaque rupture due to the exposure of sub-intima collagen with circulating and recruited platelets [Tselepis et al., 2011]. Clots extracted from occluded vessels have been evaluated in terms of fiber diameter and thickness. Clot samples were incubated for 1 hr in room temperature in a mixture of HBS, CaCl2, fibrinogen and thrombin [Dugan et al., 2006]. These observations might gain therapeutic insights. SEM allows visualization of full three-dimensional image the severely altered collagen structures of heart in temporal intervals after AMI. Ultrastructure of Infarct scar tissue and collagen fibers can be investigated in various time intervals after AMI. SEM can also used for demonstration of the pathogens suggested to be associated with progression of atherosclerosis. Presence of C. pneumonia (CP) in the cytoplasm of cardiomyocytes, with large abnormal reticular bodies surrounded by abundant mitochondria and numerous electron dense sites reflecting nucleoid condensation near the CP cell wall, are displayed using TEM [Spagnoli et al., 2007]. EM evaluation can also be applied for ultrastructural analysis of cell-to-cell contacts, basement membranes, membrane channels, receptor proteins, lipid rafts, cholesterol-rich plasma domains and plasma invaginations within acute ischemic event. Volume fraction (vV) of different tissue components and cell organelles could be quantified using stereological analysis of TEM [Lindal et al., 1990]. SEM provided with a rectilinear grid can calculate volume densities of intact and disrupted myofibrils [Sherman et al., 2000].

TEM with a standardized in vitro method can be used to evaluate the degree of blood platelet reactivity. Through this technique the number of circulating platelets/mm^3 is also determined. Three distinct types of platelets are observed when platelets are classified at the magnification level of TEM. The round type is compact, has a smooth contour, uniformly electron-dense and corresponded to the disc-shaped circulating platelet. Dendritic type is characterized by a compact, electron-dense central area from which pseudopodia extruded.

The spread type shows varying degrees of cytoplasmic spreading between adjacent pseudopodia accompanies by relocation of internal organelles. Platelet differential count includes the percent of round, dendritic and spread type platelets. Also the number of platelet aggregates counted during classification of the 100 single platelets can be recorded through this technique [Riddle et al., 1983]. TEM can also be used for acute ischemic events related to cardiotoxic compounds. TEM has potential to be used for molecular characterization of disease mechanisms involved in the development and progression of ACS. Indeed, myocardial autophagy variation and drug effects on mitochondrial function, apoptosis and in one word cytoprotection can also be seen using SEM [Zhang et al., 2009]. An example is beneficial effects of Carvedilol on mitochondrial function [Zhang et al., 2009]. EM analysis provided structural insights to the beneficial effects of Glucose-Insulin-Potassium infusion on myocardium with reduced mitochondrial flocculent granules and diminished infarct size [Sybers et al., 1973]. Effects of applied angiogenic factors, growth factors and engrafted regenerating stem cells for the treatment of ACS could be investigated using EM. TEM analysis displayed progression of cardiac progenitor cells displayed elongated uninucleated beating cells with myosin filaments radiating outward from dense bodies into an organizing sarcomer and copious mitochondria [Winitsky et al., 2005]. EM analysis provides valuable information from co-cultured stem cells with cardiomyocytes which can gain insights into the in depth understanding of regenerative medicine and its therapeutic opportunities. Characterization of cardiomyocyte progenitors and their niches is possible through application of SEM. These cells show ultrastructurally thin filaments organized by desmine-like structures, thick filaments, Z-line dense structures and confluent intracytoplasmic vesicles recognized as primordial T tubules [Popescu et al., 2009].

TEM analysis made progress in evaluation of protective effects of ischemic preconditioning (IPC) on ACS outcomes. Mitochondria isolated directly from IPC rabbit hearts showed a delayed mitochondrial pore opening by exposure to Calcium-overload [Argaud et al., 2004]. Thus less mitochondria sweltering, cristolysis and lost membrane integrity was occurred [Argaud et al., 2004]. Subsequently, improved myocardial salvage with less apoptosis and necrosis was occurred [Argaud et al., 2004]. Using EM analysis, it is possible to evaluate complications of ACS as rupture of papillary muscles, intraventricular septum and free wall by samples taken from these segments post-mortem or during reparative interventions. It is possible to observe changes made in vessels and organs remote from heart during acute coronary attacks using EM. EM can also be used for evaluation of adaptive and non-adaptive responses to acute ischemia. Myocardial hibernation is a condition that heart tries to restore an approximately normal oxygen supply/demand ratio in order to preserve myocardial viability [McFalls et al., 2007]. This is achieved by down-regulation of cardiac contractile function in response to diminished blood supply [Heusch & Schulz, 2009]. Observed ultrastructural changes in nonreperfused hibernated myocytes are altered nucleoplasm with homogenously dispersed heterochromatin and heterochromatin clumping which are consistent with adoption of dedifferentiated state resembling fetal cardiomyocytes [Borgers, 2002, Sherman et al., 2000]. Other changes include reappearance of strands of rough endoplasmic reticulum, reappearance and accretion of glycogen masses, transformed mitochondrial structure into numerous small dark and elongated mitochondria with condensed matrix, presence of large areas with non-specific cytoplasm, vacuoles, lipid droplets, lost myofibrils from perinuclear area, depletion of myocytes (myolysis) and slightly enlarged endothelial cell space [Elsässer et al., 1997, Dispersyn et al., 2001, Sherman

et al., 2000]. Loss of sarcoplasmic reticulum and T-tubules, disrupted and disassembled myofibrillar structures with apparent irregularly oriented thick filaments aggregates in perinuclear and between myofibrils, reduced sarcoplasmic A-band length without obvious scar tissue are in favor of hibernation [Borgers, 2002, Sherman et al., 2000]. The end-diastolic lengthening of subendocardial segments during flow reduction and mechanical loads determine the frequency of myofibrillar disruption [Sherman et al., 2000].

Apoptotic cell death has been shown in portions of the myocardium remote from the infarct site which is attributed to remodeling [Schwarz et al., 2006]. EM showed abundant macrophages in vulnerable lesions accompanied by lower proportion of viable SMCs [Bauriedel et al., 1999]. In these cases, macrophage apoptosis was also observed in intimal cell pool [Bauriedel et al., 1999]. Higher proportion of apoptotic SMCs in intimal cell pool is parallel with increased frequency of apoptotic remnants in ruptured and eroded plaques [Bauriedel et al., 1999]. Based on the concept of cross-talk between apoptosis and inflammatory necrosis, depletion of SMC and collagen with high density of inflammatory cells reflects incorporation of both apoptosis and necrosis pathways [Bauriedel et al., 1999]. Presence of multi-lammelated basal laminae encircling apoptotic SMCs implies loss of SMC/matrix adhesion [Bauriedel et al., 1999]. This cell detaching from surrounding extracellular matrix is so-called anoikis [Bauriedel et al., 1999]. Engulfed apoptotic bodies were observed using TEM in SMCs and macrophages [Bauriedel et al., 1999]. Paucity of cell debris on normal extracellular matrix indicates an effective sealing of apoptotic structures [Bauriedel et al., 1999]. Typical finding of cellular necrosis showed by EM include shrunken cells with marginated and clumped nuclear chromatin, disrupted cytoplasmic membranes, dispersed cytoplasmic organelles, degraded pericellular matrix, stretched fibers with wide I bands and contraction bands [Bauriedel et al., 1999, Trump et al., 1997, Ohno et al., 1998]. In these cells large round spaces with residual central structures presumably due to residual protein or lipid components of decalcified granular dense bodies have been shown in mitochondria [Kloner et al., 1974].

Generally, cell injury progresses from an initially reversible phase (pre-lethal phase) to early stage of an irreversible phase (point of return) and ultimately into end stage irreversible phase (postmortem phase) [Trump et al., 1997]. All of these three death phases have been figured out using EM, but ultrastructural features seen in reperused myocytes implicates a cell death pattern compatible with oncosis [Sayk & Bartels, 2004]. It progresses from reversible oncosis without DNA fragmentation to irreversible oncosis with or without DNA fragmentation [Makowski, 2005]. It is in contrast with early stages of apoptotic cell death which no DNA fragmentation is visible [Hwang et al., 2011]. Other ultrastructural features of ischemic-reperfusion injury include increased total volume fraction of capillaries accompanied with decreased capillary fraction of endothelial cells [Lindal et al., 1990].

2. References

Adelide University. 2011. Cryo-ultramicrotomy or Cryo-sectioning, Microscopy department of Adelide university, https://www.adelaide.edu.au/microscopy/techniques/cryoultramicrotomy.html

Abela. G., Aziz. K. & DeJong. J. (2006). Cholesterol Crystals Cause Acute Coronary Events by Perforating the Arterial Intima. Circulation. 114:II_22.

Abela GS., Aziz. K., Vedre. A., Pathak. DR., Talbott. JD. & Dejong. J. (2009). Effect of cholesterol crystals on plaques and intima in arteries of patients with acute coronary and cerebrovascular syndromes. Am J Cardiol 103:959-68.

Argaud. L., Gateau-Roesch. O., Chalabreysse. L., Gomez. L., Loufouat. J., Thivolet-Béjui. F., Robert. D. & Ovize. M. (2004). Preconditioning delays Ca2+-induced mitochondrial permeability transition. Cardiovasc Res 61:115-22.

Bauriedel. G., Hutter. R., Welsch. U., Bach. R., Sievert. H. & Lüderitz. B. (1999). Role of smooth muscle cell death in advanced coronary primary lesions: implications for plaque instability. Cardiovasc Res 41:480-8.

Bergmans. L., Moisiadis. P., Van Meerbeek. B., Quirynen. M. & Lambrechts. P. (2005). Microscopic observation of bacteria: review highlighting the use of environmental SEM. Int Endod J 38:775-88.

Bogner. A., Jouneau. PH., Thollet. G., Basset. D. & Gauthier. C. (2007). A history of scanning electron microscopy developments: towards "wet-STEM" imaging. Micron 38:390-401.

Bopassa. JC., Vandroux. D., Ovize. M. & Ferrera. R. (2006). Controlled reperfusion after hypothermic heart preservation inhibits mitochondrial permeability transition-pore opening and enhances functional recovery. Am J Physiol Heart Circ Physiol 291:H2265-71.

Buja. LM., Dees. JH., Harling. DF. & Willerson. JT. (1976). Analytical electron microscopic study of mitochondrial inclusions in canine myocardial infarcts. J Histochem Cytochem. 24:508-16.

Buja. LM., Burton KP, Hagler HK & Willerson JT. (1983). Quantitative x-ray microanalysis of the elemental composition of individual myocytes in hypoxic rabbit myocardium. Circulation 68, No. 4, 872-88.

Borgers. LM. (2002). Hibernating myocardium: Programmed cell survival or programmed cell death? Exp Clin Cardiol 7:69-72.

Luther. PK. (2007). Structural analysis of cardiac muscle by modern electron microscopy. British Society for Cardiovascular Research Bulletin, 20:4-10.

Faulkner. C., Akman. OE., Bell. K., Jeffree. C. & Oparka. K. (2008). "Peeking into Pit Fields: A Multiple Twinning Model of Secondary Plasmodesmata Formation in Tobacco". Plant Cell 20: 1504.

Dempsey. GP. & Bullivant. S. (1976). A copper block method for freezing non-cryoprotected tissue to produce ice-crystal-free regions for electron microscopy. II. Evaluation using freeze fracturing with a cryo-ultramicrotome. J Microsc 106:261-71.

Dispersyn. GD., Geuens. E., Ver Donck. L., Ramaekers. FC. & Borgers. M. (2001). Adult rabbit cardiomyocytes undergo hibernation-like dedifferentiation when co-cultured with cardiac fibroblasts. Cardiovasc Res 51(2):230-40.

Duchen. MR. (2004). Roles of mitochondria in health and disease. Diabetes 53 Suppl 1:S96-102.

Dugan. TA, Yang. VW., McQuillan. DJ. & Höök. M. (2006). Decorin modulates fibrin assembly and structure. J Biol Chem 281:38208-16.

Ehara. S., Kobayashi. Y., Yoshiyama. M., Shimada. K., Shimada. Y., Fukuda. D., Nakamura. Y., Yamashita. H., Yamagishi. H., Takeuchi. K., Naruko. T., Haze. K., Becker. AE., Yoshikawa. J. & Ueda. M. (2004). Spotty calcification typifies the culprit plaque in patients with acute myocardial infarction: an intravascular ultrasound study. Circulation 110: 3424–3429.

Elsässer. A., Schlepper. M., Klövekorn. WP., Cai. WJ., Zimmermann. R., Müller. KD., Strasser. R., Kostin. S., Gagel. C., Münkel. B., Schaper. W. & Schaper. J. (1997). Hibernating myocardium: an incomplete adaptation to ischemia. Circulation. 96:2920-31.

Erni. R., Rossell. MD., Kisielowski. C. & Dahmen. U. (2009). Atomic-resolution imaging with a sub-50-pm electron probe. Phys Rev Lett 102:096101.

Ewence. AE., Bootman. M., Roderick. HL., Skepper. JN., McCarthy. G., Epple. M., Neumann. M., Shanahan. CM. & Proudfoot. D. (2008). Calcium phosphate crystals induce cell death in human vascular smooth muscle cells: a potential mechanism in atherosclerotic plaque destabilization. Circ Res 103:e28-34.

Guyton.JR. & Klemp. KF. (1992). Early extracellular and cellular lipid deposits in aorta of cholesterol-fed rabbits. Am J Pathol 141:925-36.

Hagler. HK & Buja. LM. (1986). Effect of specimen preparation and section transfer techniques on the preservation of ultrastructure, lipids and elements in cryosections. Journal of Microscopy 141: 311–317,

Hwang. B., Hwang. JS., Lee. J., Kim. JK., Kim. SR., Kim. Y. & Lee. DG. (2011). Induction of yeast apoptosis by an antimicrobial peptide, Papiliocin. Biochem Biophys Res Commun 408:89-93.

Heusch G & Schulz R. (2009) Hibernation or repetitive stunning – does it matter? The basic perspective Heart Metab 42:32–33

Hindmarsh. JP., Russell. AB. & Chen XD. (2007). "Fundamentals of the spray freezing of foods—microstructure of frozen droplets". Journal of Food Engineering 78: 136–150.

Hüser. J., Rechenmacher. CE. & Blatter. LA. (1998). Imaging the permeability pore transition in single mitochondria. Biophys J 74:2129-37.

Hoffstein. S., Gennaro. DE., Weissmann. G., Hirsch. J., Streuli. F. & Fox. AC. (1975). Cytochemical localization of lysosomal enzyme activity in normal and ischemic dog myocardium. Am J Pathol 79:193-206.

Ishidi E, Adamu I, Kolawale E, Sunmonu K & Yakubu M. (2011). Morphology and Thermal Properties of Alkaline Treated Palm Kernel Nut Shell – HDPE Composites. Journal of Emerging Trends in Engineering and Applied Sciences (JETEAS) 2 (2): 346-350

Jerome. WG., Lewis. JC., Taylor. RG. & White. MS. (1983). Concurrent endothelial cell turnover and leukocyte margination in early atherosclerosis. Scan Electron Microsc Pt 3:1453-9.

KAMARI. Y., Cohen. H., Shaish. A., Bitzur. R., Afek. A., Shen. S., Vainshtein. A. & Harats. D. (2008). Characterisation of atherosclerotic lesions with scanning electron microscopy (SEM) of wet tissue. Diab Vasc Dis Res 5:44-7.

Karnovsky. MJ. (1965). "A formaldehyde-glutaraldehyde fixative of high osmolality for use in electron microscopy". Journal of Cell Biology 27: 137A.

Kawamura. K., Cowley. MJ., Karp. RB., Mantle. JA., Logic. JR., Rogers. WJ., Russel RO., Rackley. CE. & Tames. TN. (1978). Intramitochondrial inclusions in the myocardial cells of human hearts and coronary disease. J Mol Cell Cardiol 10:797-811.

Kiernan. JA. (2000). "Formaldehyde, formalin, paraformaldehyde and glutaraldehyde: What they are and what they do". Microscopy Today: 8–12.

Kloner. RA., Ganote. CE., Whalen D, Jennings. RB. (1974). Effect of a transient period of ischemia on myocardial cells. II. Fine Structture During the First Few Minutes of Reflow. Am J Pathol. 1974 Mar;74(3):399-422.

Li YY, Chen D, Watkins SC & Feldman AM (2001). Mitochondrial abnormalities in tumor necrosis factor-alpha-induced heart failure are associated with impaired DNA repair activity. Circulation 104:2492-7.

Lindal. S., Gunnes. S., Ytrehus. K., Straume BK., Jørgensen. L. & Sørlie. D. (1990). Amelioration of reperfusion injury following hypothermic, ischemic cardioplegia in isolated, infarcted rat hearts. Eur J Cardiothorac Surg 4:33-9.

Maco. B., Mandinova. A., Dürrenberger. MB., Schäfer. BW., Uhrík. B. & Heizmann. CW. (2001). Ultrastructural distribution of the S100A1 Ca2+-binding protein in the human heart. Physiol Res 50:567-74.

Makowski. G. (2005). Advances in Clinical Chemistry, 40, p45, Academic Press, ISBN: 0120103400

Mancuso. J., Maxwell. W. & Danilatos. G. (1988). Secondary Electron Detector for Use in a Gaseous Atmosphere", US patent 4785182 11:15McFalls. EO., Kelly. RF., Hu. Q., Mansoor. A., Lee. J., Kuskowski. M., Sikora. J., Ward. HB. & Zhang. J. (2007). The energetic state within hibernating myocardium is normal during dobutamine despite inhibition of ATP-dependent potassium channel opening with glibenclamide. Am J Physiol Heart Circ Physiol 293:H2945-51.

McMullan. D. (1993). "Scanning Electron Microscopy, 1928–1965". 51st Annual Meeting of the Microscopy Society of America. Cincinnati, OH.

Mohankumar D.2010. Environmental Scanning Electron Microscope –ESEM: *wordpress.*

Nadra. I., Boccaccini. AR., Philippidis. P., Whelan. LC., McCarthy. GM., Haskard. DO. & Landis. RC. (2008). Effect of particle size on hydroxyapatite crystal-induced tumor necrosis factor alpha secretion by macrophages. Atherosclerosis. 196: 98–105.

Ohno. M., Takemura. G., Ohno. A., Misao. J., Hayakawa. Y., Minatoguchi. S., Fujiwara. T. & Fujiwara. H. (1998). "Apoptotic" myocytes in infarct area in rabbit hearts may be oncotic myocytes with DNA fragmentation: analysis by immunogold electron microscopy combined with In situ nick end-labeling. Circulation 98:1422-30.

Osumi. M., Konomi. M., Sugawara. T., Takagi. T. & Baba. M. (2006). High-pressure freezing is a powerful tool for visualization of Schizosaccharomyces pombe cells: ultra-low temperature and low-voltage scanning electron microscopy and immunoelectron microscopy. J Electron Microsc (Tokyo) 55:75-88.

Park. JS., Gamboni-Robertson. F., He. Q., Svetkauskaite. D., Kim. JY., Strassheim. D., Sohn. JW., Yamada. S., Maruyama. I., Banerjee. A., Ishizaka. A. & Abraham. E. (2006). High mobility group box 1 protein interacts with multiple Toll-like receptors. Am J Physiol Cell Physiol 290: C917–924.

Peine. CJ.& Low. FN. (1975) Scanning electron microscopy of cardiac endothelium of the dog. Am J Anat 142:137-57.

Popescu. LM., Gherghiceanu. M., Manole. CG. & Faussone-Pellegrini. MS. (2009). Cardiac renewing: interstitial Cajal-like cells nurse cardiomyocyte progenitors in epicardial stem cell niches. J Cell Mol Med 13:866-86.

ProSciTech: Critical point dryers, freeze dryers".
http://www.proscitech.com/cataloguex/online.asp

Porto. A., Palumbo. R., Pieroni. M., Aprigliano. G., Chiesa. R., Sanvito. F., Maseri. A. & Bianchi. ME. (2006). Smooth muscle cells in human atherosclerotic plaques secrete and proliferate in response to high mobility group box 1 protein. Faseb J 20: 2565–2566.

Proudfoot. D., Skepper. JN., Hegyi. L., Bennett. MR., Shanahan. CM. & Weissberg. (2000). PL. Apoptosis regulates human vascular calcification in vitro: evidence for initiation of vascular calcification by apoptotic bodies. Circ Res. 87: 1055–1062.

Rajapakse. S., Rodrigo. PC. & Selvachandran. J. (2010). Management of acute coronary syndrome in a tertiary care general medical unit in Sri Lanka: how closely do we follow the guidelines? J Clin Pharm Ther 35:421-7.

Rame. JE., Barouch. LA., Sack. MN., Lynn. EG., Abu-Asab. M., Tsokos. M., Kern. SJ., Barb. JJ., Munson. PJ., Halushka. MK., Miller. KL., Fox-Talbot. K., Zhang. J., Hare. JM., Solomon. MA. & Danner. RL. (2011). Caloric restriction in leptin deficiency does not correct myocardial steatosis: failure to normalize PPAR{alpha}/PGC1{alpha} and thermogenic glycerolipid/fatty acid cycling. Physiol Genomics 43:726-38.

Read. ND. & Jeffree. CE. (1991). Low-temperature scanning electron microscopy in biology. J Microsc 161:59-72.

Riddle. JM., Stein. PD., Magilligan. DJ. & McElroy. HH. (1983). Evaluation of platelet reactivity in patients with valvular heart disease. J Am Coll Cardiol. 1983 Jun;1(6):1381-4.

Russell. FD., Skepper. JN. & Davenport. AP. (1998). Evidence Using Immunoelectron Microscopy for Regulated and Constitutive Pathways in the Transport and Release of Endothelin. Journal of Cardiovascular Pharmacology: 31: 424-430

Sætersdal. TS., Myklebust. R., Engedal. H. & Ødegaarden. S. (1978). Substructure of inner mitochondrial membranes of myocardial cells as shown by cryo-ultramicrotomy. Cell and Tissue Research 186:13-24

Sage MD & Jennings RB (1988). Cytoskeletal injury and subsarcolemmal bleb formation in dog heart during in vitro total ischemia. Am J Pathol 133:327-37.

Sayk. F. & Bartels. C. (2004). Oncosis rather than apoptosis? Ann Thorac Surg 77:382; author reply 382-3.

Schatten H. & Pawley J. (2007). Biological Low-Voltage Scanning Electron Microscopy. Springer 61–63.

Schwarz. K., Simonis. G., Yu. X., Wiedemann. S. & Strasser. RH. (2006). Apoptosis at a distance: remote activation of caspase-3 occurs early after myocardial infarction. Mol Cell Biochem 281:45-54.

Sekiya. T., Kitajima. Y. & Nozawa. Y. (1979). Effects of lipid-phase separation on the filipin action on membranes of ergosterol-replaced Tetrahymena cells, as studied by freeze-fracture electron microscopy. Biochim Biophys Acta 550:269-78.

Severs. N. (2007). Freeze-fracture electron microscopy, Nature Protocols 2, -547 - 576 (2007)

Mitsuoka. K. (2011). Obtaining high-resolution images of biological macromolecules by using a cryo-electron microscope with a liquid-helium cooled stage. Micron 42:100-6.

Sherman. AJ., Klocke. FJ., Decker. RS., Decker. ML., Kozlowski. KA., Harris. KR., Hedjbeli. S., Yaroshenko. Y., Nakamura. S., Parker. MA., Checchia. PA. & Evans. DB. (2000). Myofibrillar disruption in hypocontractile myocardium showing perfusion-contraction matches and mismatches. Am J Physiol Heart Circ Physiol 278:H1320-34.

Schmid. K., McSharry. WO., Pameijer. CH. & Binette. JP. (1980). Chemical and physicochemical studies on the mineral deposits of the human atherosclerotic aorta. Atherosclerosis 37: 199–210

Sojitra P, Engineer Ch, Raval A, Kothwala D, Jariwala A, Kotadia H, Adeshara S & Mehta G. (2009). Surface Enhancement and Characterization of L-605 Cobalt Alloy Cardiovascular Stent by Novel Electrochemical Treatment. Trends Biomater. Artif. Organ 23:55-64.

Spagnoli. LG., Pucci. S., Bonanno. E., Cassone. A., Sesti. F., Ciervo. A. & Mauriello. A. (2007). Persistent Chlamydia pneumoniae infection of cardiomyocytes is correlated with fatal myocardial infarction. Am J Pathol 170:33-42.

Sun. W., Zheng. L. & Huang. L. (2011). Role of unusual CD4 (+) CD28 (-) T cells in acute coronary syndrome. Mol Biol Rep 22.

Suzuki. E. (2002). "High-resolution scanning electron microscopy of immunogold-labelled cells by the use of thin plasma coating of osmium". Journal of Microscopy 208: 153–157.

Sybers. HD., Maroko. PR., Ashraf. M., Libby. P. & Braunwald. E. (1973). The effect of glucose-insulin-potassium on cardiac ultrastructure following acute experimental coronary occlusion. Am J Pathol 70:401-20.

Toumpoulis. IK., Oxford. JT., Cowan. DB., Anagnostopoulos. CE., Rokkas. CK., Chamogeorgakis. TP., Angouras. DC., Shemin. RJ., Navab. M., Ericsson. M., Federman. M., Levitsky. S. & McCully. JD. (2009). Differential expression of collagen type V and XI alpha-1 in human ascending thoracic aortic aneurysms. Ann Thorac Surg 88:506-13.

Tran. PK., Tran-Lundmark. K., Soininen. R., Tryggvason. K., Thyberg. J. & Hedin. U. (2004). Increased intimal hyperplasia and smooth muscle cell proliferation in transgenic mice with heparan sulfate-deficient perlecan. Circ Res 94:550-8.

Trump. BF., Berezesky. IK., Chang. SH. & Phelps. PC. (1997). The pathways of cell death: oncosis, apoptosis, and necrosis. Toxicol Pathol 25:82-8.

Tselepis. AD., Gerotziafas. G., Andrikopoulos. G., Anninos. H. & Vardas. P. (2011). Mechanisms of platelet activation and modification of response to antiplatelet agents. Hellenic J Cardiol 52:128-40.

Ueno. M., Suzuki. J., Zenimaru. Y., Takahashi. S., Koizumi. T., Noriki. S., Yamaguchi. O., Otsu. K., Shen. WJ., Kraemer. FB. & Miyamori. I. (2008). Cardiac overexpression of hormone-sensitive lipase inhibits myocardial steatosis and fibrosis in streptozotocin diabetic mice. Am J Physiol Endocrinol Metab 294:E1109-18.

Vengrenyuk. Y., Carlier. S., Xanthos. S., Cardoso. L., Ganatos. P., Virmani. R., Einav. S., Gilchrist. L. & Weinbaum. S. (2006). A hypothesis for vulnerable plaque rupture due to stress-induced debonding around cellular microcalcifications in thin fibrous caps. Proc Natl Acad Sci U S A 103: 14678–14683.

Virchow. R. (1860). A more precise account of fatty metamorphosis. In: Chance F, ed. Cellular Pathology. London, Gryphonham 342–366

Virmani. R, Burke. AP., Kolodgie. FD. & Farb. A. (2003). Pathology of the thin-cap fibroatheroma: a type of vulnerable plaque. J Interv Cardiol 16: 267–272.

Vye MV & Fischman DA (1970). The morphological alteration of particulate glycogen by en bloc staining with uranyl acetate. J Ultrastruct Res 33:278-91.

Wiemer M, Butz T, Schmidt W, Schmitz KP, Horstkotte D, Langer C. Scanning electron microscopic analysis of different drug eluting stents after failed implantation: from nearly undamaged to major damaged polymers. Catheter Cardiovasc Interv. 2010 May 1;75(6):905-11.

Winitsky. SO., Gopal. TV., Hassanzadeh. S., Takahashi. H., Gryder. D., Rogawski. MA., Takeda. K., Yu. ZX., Xu. YH. & Epstein. ND. (2005). Adult murine skeletal muscle contains cells that can differentiate into beating cardiomyocytes in vitro. PLoS Biol 3:e87.

www.upesh.edu.pk/academics/researchcenter

Zhang. JL., Lu. JK., Chen. D., Cai. Q., Li. TX., Wu. LS. & Wu. XS. (2009). Myocardial autophagy variation during acute myocardial infarction in rats: the effects of carvedilol. Chin Med J (Engl) 122:2372-9.

Zhou. Z., Han. JY., Xi. CX., Xie. JX., Feng. X., Wang. CY., Mei. L. & Xiong. WC. (2008). HMGB1 regulates RANKL-induced osteoclastogenesis in a manner dependent on RAGE. J Bone Miner Res 23: 1084–1096.

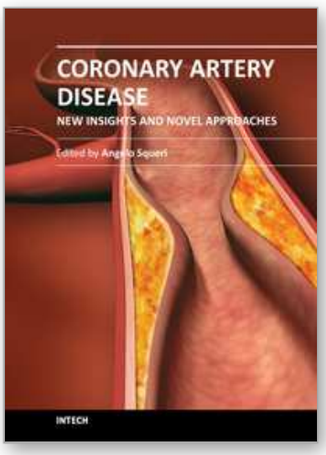

Coronary Artery Disease - New Insights and Novel Approaches
Edited by Dr. Angelo Squeri

ISBN 978-953-51-0344-8
Hard cover, 260 pages
Publisher InTech
Published online 16, March, 2012
Published in print edition March, 2012

Coronary Artery disease is one of the leading causes of death in industrialized countries and is responsible for one out of every six deaths in the United States. Remarkably, coronary artery disease is also largely preventable. The biggest challenge in the next years is to reduce the incidence of coronary artery disease worldwide. A complete knowledge of the mechanisms responsible for the development of ischaemic heart disease is an essential prerequisite to a better management of this pathology improving prevention and therapy. This book has been written with the intention of providing new concepts about coronary artery disease pathogenesis that may link various aspects of the disease, going beyond the traditional risk factors.

InTech Europe
University Campus STeP Ri
Slavka Krautzeka 83/A
51000 Rijeka, Croatia
Phone: +385 (51) 770 447
Fax: +385 (51) 686 166
www.intechopen.com

InTech China
Unit 405, Office Block, Hotel Equatorial Shanghai
No.65, Yan An Road (West), Shanghai, 200040, China
中国上海市延安西路65号上海国际贵都大饭店办公楼405单元
Phone: +86-21-62489820
Fax: +86-21-62489821

IntechOpen